L	X	Compound	Reference
tpy	CN^-	**1a**	[9]
	NCS^-	**2a**	[9]
	$(\mu\text{-NC})Fe^{III}(CN)_5$	**3a**	[9]
	$(\mu\text{-NC})Fe^{II}(CN)_5$	**3a^r**	[9]
	$(\mu\text{-NC})Cr^{III}(CN)_5$	**4a**	[9]
	$(\mu\text{-NC})Ru^{II}(CN)_5$	**5a^r**	**this work**
	$(\mu\text{-NC})Os^{III}(CN)_5$	**6a**	**this work**
	$(\mu\text{-NC})Os^{II}(CN)_5$	**6a^r**	**this work**
	$(\mu\text{-NC})Ru(py)_4(CN)$	**7a^r**	**this work**
tpm	CN^-	**1b**	[9]
	NCS^-	**2b**	[9]
	$(\mu\text{-NC})Fe^{III}(CN)_5$	**3b**	[9]
	$(\mu\text{-NC})Fe^{II}(CN)_5$	**3b^r**	[9]
	$(\mu\text{-NC})Cr^{III}(CN)_5$	**4b**	[9]
	$(\mu\text{-NC})Ru^{II}(CN)_5$	**5b^r**	**this work**
	$(\mu\text{-NC})Os^{III}(CN)_5$	**6b**	**this work**
	$(\mu\text{-NC})Os^{II}(CN)_5$	**6b^r**	**this work**
	$(\mu\text{-NC})Ru(py)_4(CN)$	**7b^r**	**this work**

Table S1. Complexes of the formula [Ru(L)(bpy)(X)] studied in this work.

Compound	**6a**	**7a^r**	**6b**
Empirical Formula	$C_{55}H_{39}N_{11}O_{4.5}PRuOs$	$C_{47}H_{38}N_{11}O_3P_2F_{12}Ru_2$	$C_{50}H_{38}N_{14}O_5PRuOs$
fw / g mol^{-1}	1248,21	1296,96	1237,18
T / K	298 (2)	298 (2)	298 (2)
λ / Å	0,71069	0,71069	0,71069
Cell	triclinic	monoclinic	triclinic
Space Group	P-1	P121/n1	P-1
a / Å	12,9482(5)	13,8415(11)	11,1651(3)
b / Å	13,3888(5)	17,7504(11)	13,4550(3)
c / Å	17,3370(6)	22,213(2)	19,2621(5)
α / °	101,641(3)	90,0	88,288(2)
β / °	96,360(3)	101,602(9)	76,516(2)
γ / °	114,494(4)	90,0	81,877(2)
V / Å^3	2614,29(17)	5346,1(6)	2785,67(12)
Z	2	4	2
$dens._{calc}$	1,586	1,611	1,475
μ (abs. coef.) / mm^{-1}	2,805	0,718	2,634
final index (R1)	0,0375	0,0998	0,0491
I>2σ(I) (wR2)	0,0993	0,2135	0,1006
all data (R1)	0,0535	0,2242	0,1126
all data (wR2)	0,1113	0,2951	0,1105

Table S2. Crystallographic data for compounds **6a-b** and **7a^r**.

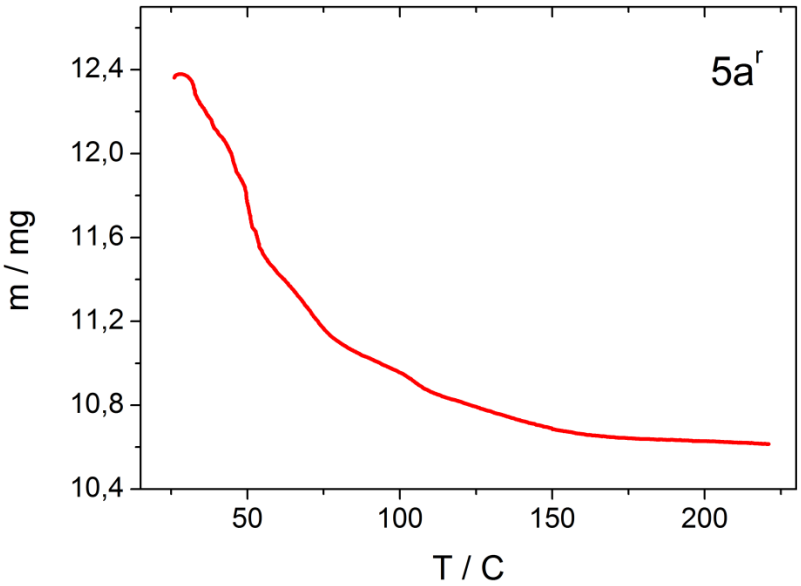

Figure S1. Thermogravimetric analysis for complex **5a**^{r}. Initial mass = 12.38 mg. Final mass = 10.62 mg. Loss = 14%.

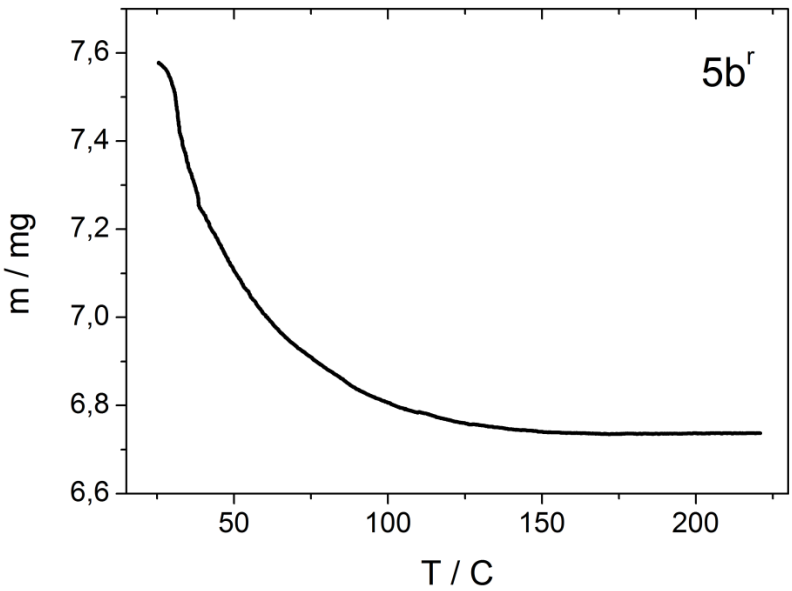

Figure S2. Thermogravimetric analysis for complex **5b**^{r}. Initial mass = 7.58 mg. Final mass = 6.74 mg. Loss = 11%.

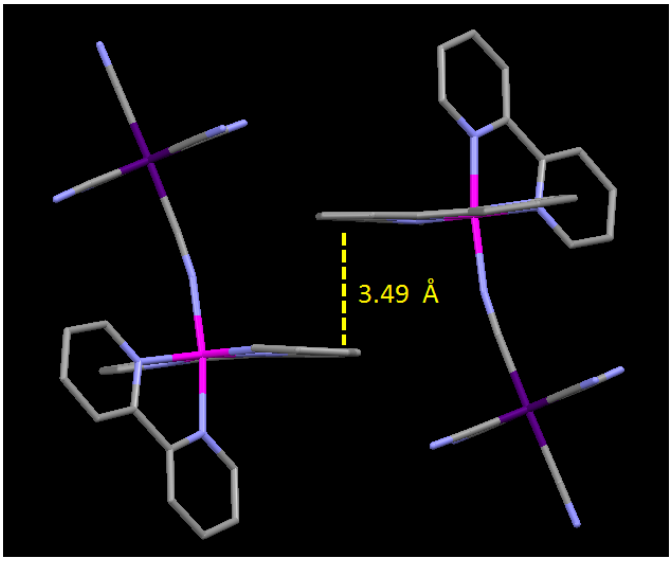

Figure S3. Tpy - tpy π stacking interactions in the crystal structure of **6a**. Hydrogen atoms, counter ions, and solvent molecules were omitted for clarity.

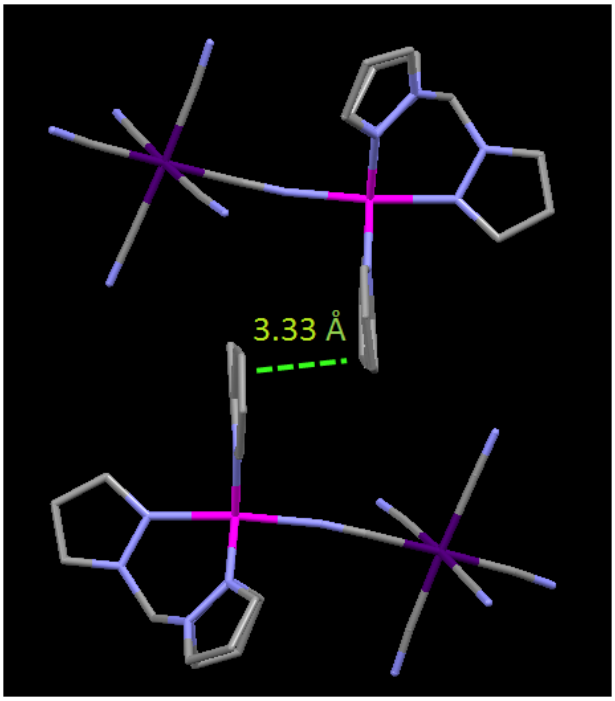

Figure S4. Bpy - bpy π stacking interactions in the crystal structure of **6b**. Hydrogen atoms, counter ions, and solvent molecules were omitted for clarity.

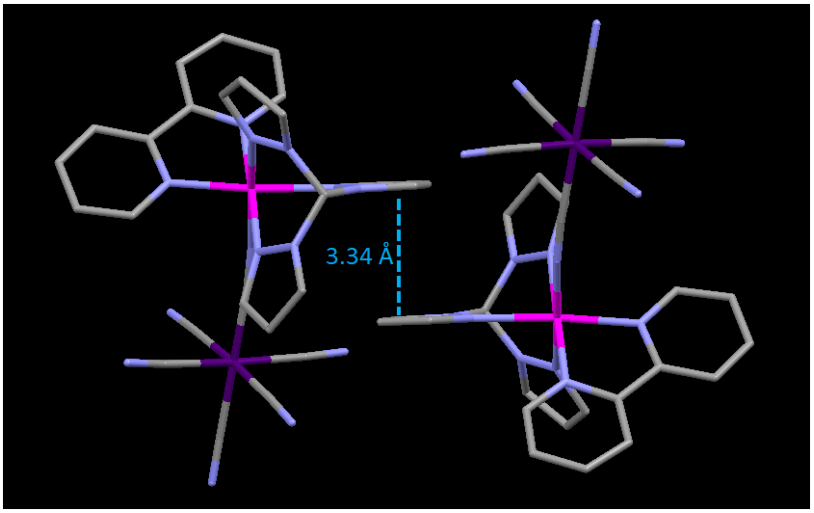

Figure S5. Tpm - tpm π stacking interactions in the crystal structure of **6b**. Hydrogen atoms, counter ions, and solvent molecules were omitted for clarity.

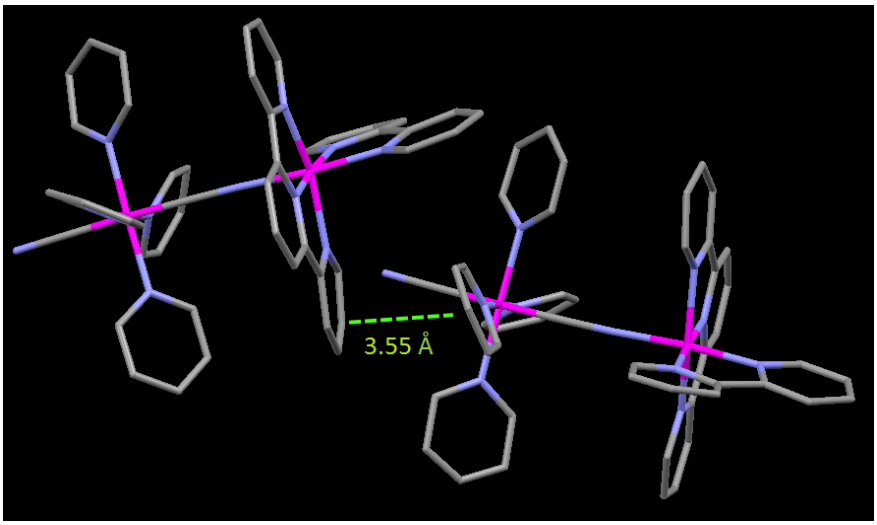

Figure S6. Tpy - py π stacking interactions in the crystal structure of **7a**^{r}. Hydrogen atoms, counter ions, and solvent molecules were omitted for clarity.

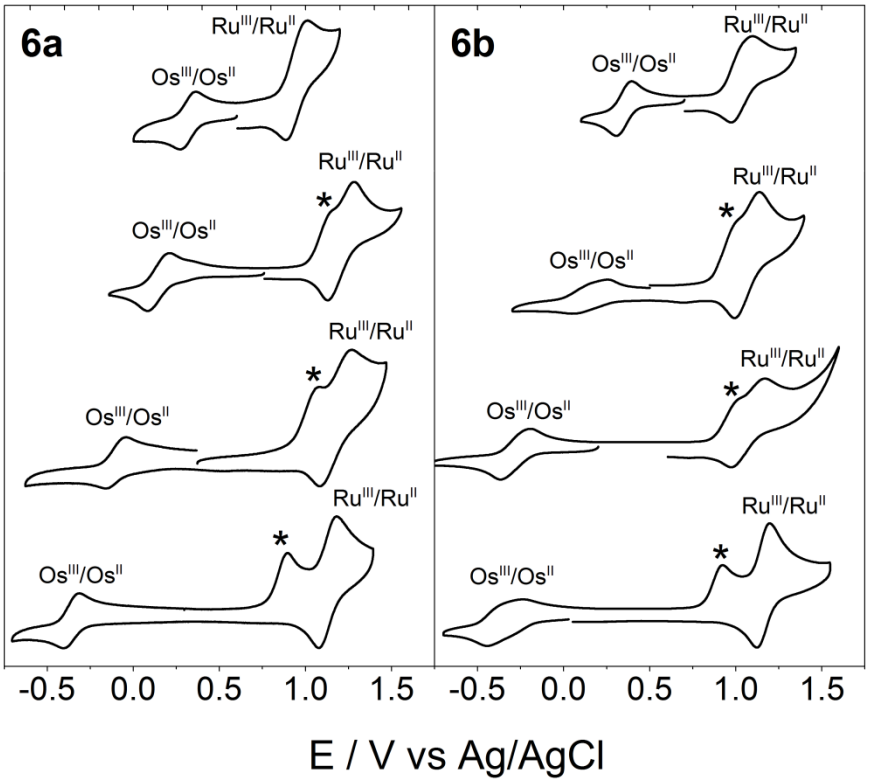

Figure S7. Electrochemistry of **6a-b** in water, methanol, ethanol and acetonitrile (from top to bottom). The wave labeled with a (*) is preliminarly assigned to a Os^{IV}/Os^{III} process.

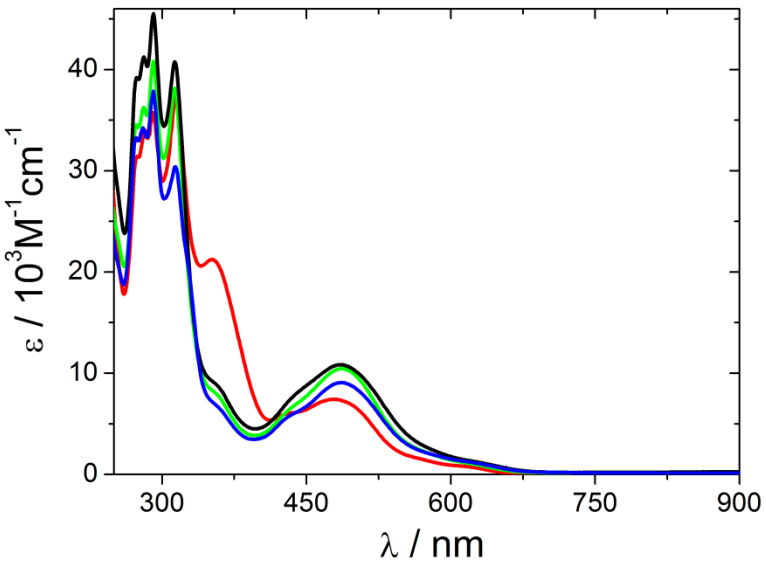

Figure S8. UV-vis absorption of the complexes **5a**^{r} (green), and **6a**^{r} (black) in water and **7a**^{r} in acetonitrile (red). For comparison purposes the spectrum of $[Ru(tpy)(bpy)(NCS)]^+$ in acetonitrile (blue) is also included.

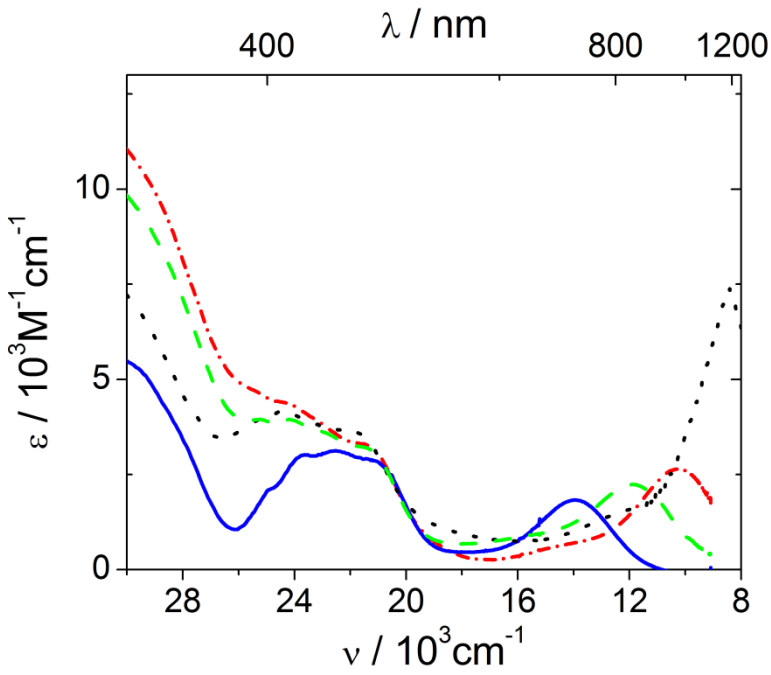

Figure S9. Vis-NIR absorption of the complexes **6b** in water (black dotted line), methanol (red dash-dotted), ethanol (green dashed line) and acetonitrile (blue solid line).

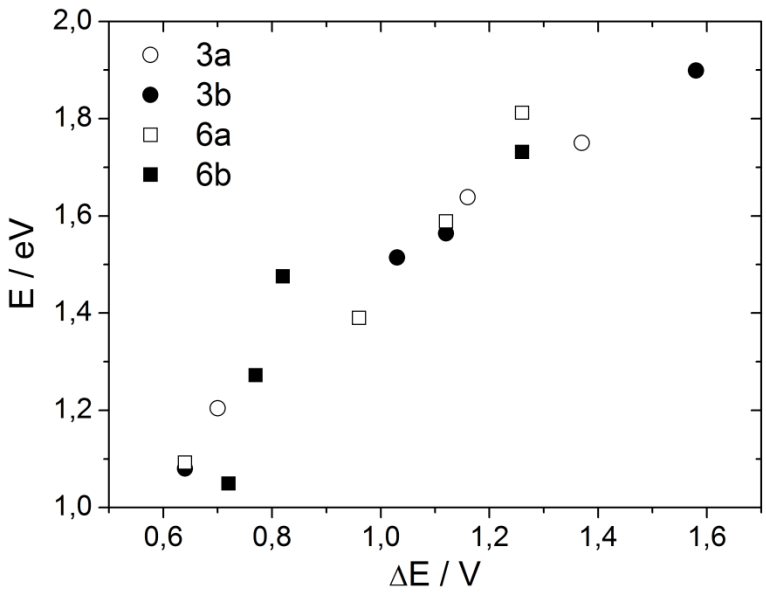

Figure S10. Correlation between the energy of the MM'CT band and the difference in the redox potentials of iron and ruthenium centers for compounds **3a-b**,[9] and **6a-b** in water, MeOH, EtOH and ACN.

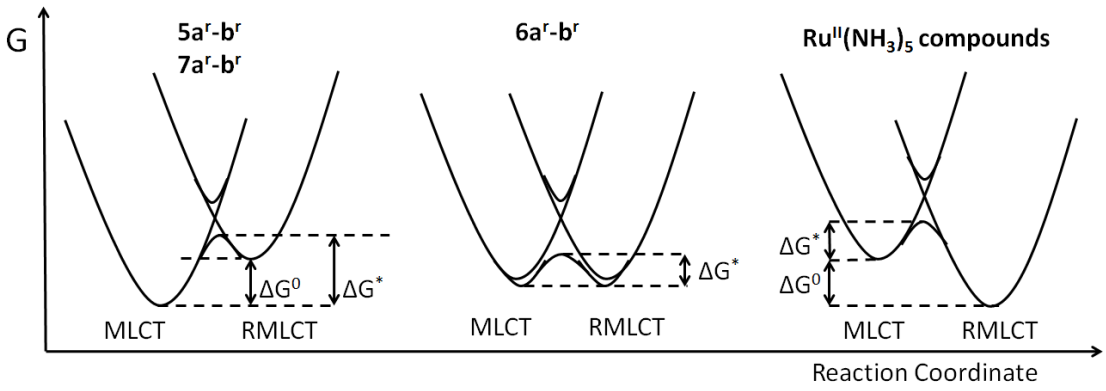

Figure S11. Excited state electron transfer energetics for complexes **5a^r-b^r**, **6a^r-b^r** and **7a^r-b^r**. $Ru(NH_3)_5$ compounds are shown for comparison purposes.

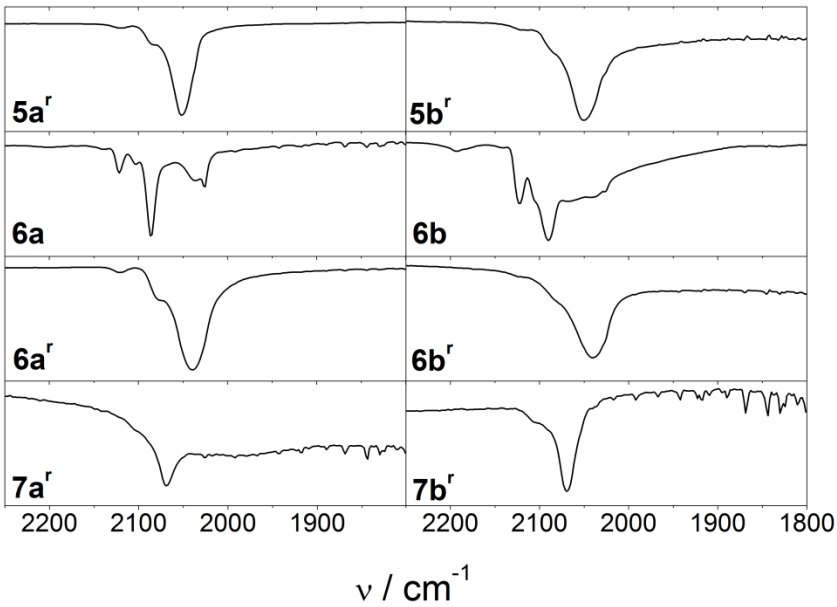

Figure S12. IR spectra in KBr pellets of **5a^r-b^r**, **6a-b**, **6a^r-b^r** and **7a^r-b^r**, from top to bottom.